THE JOURNAL OF BIOLOGICAL CHEMISTRY
Vol. 278, No. 40, Issue of October 3, pp. 38715–38722, 2003
Printed in U.S.A.

A Direct Interaction between Transforming Growth Factor (TGF)-βs and Amyloid-β Protein Affects Fibrillogenesis in a TGF-β Receptor-independent Manner*

Received for publication, April 17, 2003, and in revised form, June 30, 2003
Published, JBC Papers in Press, July 16, 2003, DOI 10.1074/jbc.M304080200

Darrell D. Mousseau‡§¶, Sarah Chapelsky§‖, Gregory De Crescenzo§, Marina D. Kirkitadze, Joanne Magoon§, Sadayuki Inoue‡‡, David B. Teplow**, and Maureen D. O'Connor-McCourt§ §§**

*From the ‡Cell Signaling Group, Neuropsychiatry Research Unit, Department of Psychiatry, University of Saskatchewan, Saskatoon S7N 5E4, Canada, the §Receptor, Signaling, and Proteomics Group, Health Sector, Biotechnology Research Institute, Montreal H4P 2R2, Canada, the **Department of Neurology, Harvard Medical School, and Center for Neurologic Diseases, Brigham & Women's Hospital, Boston, Massachusetts 02115, and the ‡‡Department of Anatomy and Cell Biology, McGill University, Montreal H3A 2B2, Canada*

Transforming growth factor-β (TGF-β) receptor-mediated signaling has been proposed to mediate both the beneficial and deleterious roles for this cytokine in amyloid-β protein (Aβ) function. In order to assess receptor dependence of these events, we used PC12 cell cultures, which are devoid of TGF-β receptors. Surprisingly, TGF-β potentiated the neurotoxic effects of the 40-residue Aβ peptide, Aβ-(1–40), in this model suggesting that there may be a direct, receptor-independent interaction between TGF-β and Aβ-(1–40). Surface plasmon resonance confirmed that TGF-β binds with high affinity directly to Aβ-(1–40) and electron microscopy revealed that TGF-β enhances Aβ-(1–40) oligomerization. Immunohistochemical examination of mouse brain revealed that hippocampal CA1 and dentate gyrus, two regions classically associated with Aβ-mediated pathology, lack TGF-β Type I receptor immunoreactivity, thus indicating that TGF-β receptor-mediated signaling would not be favored in these regions. Our observations not only provide for a unique, receptor-independent mechanism of action for TGF-β, but also help to reconcile the literature interpreting the role of TGF-β in Aβ function. These data support a critical etiological role for this mechanism in neuropathological amyloidoses.

The 39–43-mer amyloid-β (Aβ)[1] peptide is derived from the membrane-bound amyloid precursor protein (APP) as an aberrant cleavage product (1). Transgenic APP mouse models exhibit age-related extracellular amyloid deposits (plaques) and neurodegeneration as well as cerebral amyloid angiopathy (CAA) comparable to that found in human Alzheimer's disease (AD) brain (2, 3). These same models respond to both active and passive immunization against Aβ as evidenced by the reduction in levels of Aβ, the prevention and/or clearance of amyloid plaques, and the improvement in cognitive behavior (4). However, an effective preparation free of significant side effects in humans is still awaited. Indeed, clinical trials involving Aβ vaccination have been discontinued following the development of inflammation in patients brains (5). Cerebral microhemmorhaging has also been observed in similarly immunized mice (6). Although it has been suggested that antibodies capable of recognizing other Aβ epitopes or conformations should be screened (6), perhaps a closer examination of modulators of Aβ fibrillogenesis may reveal a target better suited for immunotherapy.

Among the modulators proposed to date, which include apolipoprotein E, cholesterol, and α2-macroglobulin, we were particularly interested in the cytokine transforming growth factor-β (TGF-β). The TGF-β1 isoform was recently implicated as a co-factor for amyloid deposition with the observation that cerebrovascular amyloid deposits, which are strikingly similar to those seen in patients with AD and CAA, and the ensuing neuropathological development are accelerated in bigenic mice overexpressing both TGF-β1 and human APP (hAPP), relative to hAPP transgenic mice controls (7). These authors suggested that cerebrovascular amyloid deposition might reflect TGF-β receptor-mediated induction of extracellular matrix deposition. Aβ binding proteins within these extracellular matrix components could enhance the formation and/or stability of Aβ fibrils (8, 9). A link between TGF-β and Aβ deposition was already being considered following the localization of TGF-β immunoreactivity to senile plaques and neurofibrillary tangle-bearing neurons in AD patient brain (7, 10). TGF-βs had also been shown to enhance the formation of amyloid deposits in rats when co-injected intracerebroventricularly with Aβ-(1–40) (11) and to increase the number of Aβ plaque-like deposits in hippocampal slice culture in a subfield-selective manner (12). Finally, APP production and Aβ-(1–40)/Aβ-(1–42) processing were promoted by TGF-β1 in transgenic mice (13).

In contrast to its role as a risk factor, TGF-β1 facilitates Aβ clearance and plaque burden reduction following activation of parenchymal glial cells in TGF-β1/hAPP bigenic mouse brain (14). TGF-βs have also been shown to protect neuronal cell cultures against Aβ-mediated insult (15–17) as a direct consequence of TGF-β Type II receptor activation (17).

These apparently opposing actions of TGF-β in the brain illustrate the multifunctionality of this cytokine and the dependence of its effects on the specific cellular context in which it is expressed. Additional investigation is needed to characterize the cellular and molecular processes that underlie the ef-

* This work was supported, in part by Neuropsychiatry Research Unit Establishment funds (to D. D. M.) and by the National Research Council (Canada). The costs of publication of this article were defrayed in part by the payment of page charges. This article must therefore be hereby marked "*advertisement*" in accordance with 18 U.S.C. Section 1734 solely to indicate this fact.

¶ To whom correspondence may be addressed. Tel.: 306-966-8824; Fax: 306-966-8830; E-mail: darrell.mousseau@usask.ca.

‖ Supported by the NRC Women in Engineering and Science Program.

§§ To whom correspondence may be addressed. Tel.: 514-496-6382; E-mail: maureen.o'connor@nrc.ca.

[1] The abbreviations used are: Aβ, amyloid-β; TGF, transforming growth factor; MTT, 4,5-dimethylthiazol-2-yl)-2,5-diphenyl tetrazolium.

fects of TGF-β during Aβ-mediated pathology. To date, the actions of TGF-β have centered on receptor-mediated events. In this report, we demonstrate a direct interaction between TGF-β and Aβ that promotes Aβ fibrillogenesis and neurotoxicity. Our data support a role for a unique, receptor-independent mode of action for TGF-β and define a new molecular point of intervention for inhibiting Aβ fibrillogenesis.

MATERIALS AND METHODS

TGF-β Receptor Competition Assays—Mink lung epithelial Mv1Lu cells (ATCC: CCL-64) were seeded at 2×10^5 cells/ml in Dulbecco's modified Eagle's medium (DMEM) containing 10% fetal bovine serum (FBS) for 24 h at 37 °C (5% CO_2). Cell surface receptors were cross-link-labeled with 200 pM ^{125}I-TGF-β1 (PerkinElmer Life Science Products) in the presence of increasing concentrations (1–50 μM) of Aβ-(1–40), Aβ-(25–35), and Aβ-(12–28) (BIOSOURCE, Camarillo, CA). Bis(sulfosuccinimidyl) suberate (Pierce) was used as the cross-linking reagent, and the receptors were analyzed by 4–11% gradient SDS-PAGE and autoradiography. Signal intensities were quantitated using the ImageQuaNT system (Molecular Dynamics, Sunnyvale, CA).

Circular Dichroism Spectroscopy (CD)—Aβ-(1–40) was prepared by dissolution into 50 mM phosphate buffer (pH 7.0) to yield a final concentration of 1 mg/ml. Samples were incubated at ambient temperature (22 °C) without stirring and CD measurements (at 22 °C) were performed periodically using a 0.1 cm pathlength quartz cell (Hellma, Forest Hills, NY) and an Aviv Model 62A DS spectropolarimeter (Aviv Associates, Lakewood, NJ). The scan rate was 1 nm/sec at a bandwidth of 1 nm. Three independent sets of experiments, each comprised of triplicate scans performed from 250–198 nm, were done. The buffer spectrum was subtracted from the scans and the resulting functions were smoothed. Data could not be acquired at wavelengths lower than 198 nm due to saturation of the photomultiplier. However, this range is sufficient to accurately evaluate the secondary structure state of the samples (18). Protein concentrations were determined *a posteriori* by quantitative amino acid analysis, thus enabling accurate calculation of molar ellipticities (Θ).

Neurotoxicity Assay—Rat pheochromocytoma PC12 cells (ATCC: CRL-1721) were cultured on rat tail collagen-coated plates. Both PC12 cells and human neuroblastoma SH-SY5Y cells (ATCC: CRL-2266) were maintained in Dulbecco's modified Eagle's medium containing 10% horse serum (PC12) and 5% fetal bovine serum (PC12 & SH-SY5Y) at 37 °C (5% CO_2). Cells (5×10^3/well) were differentiated to a neuronal phenotype using 100 ng/ml of NGF. The toxicity of Aβ-(1–40) was determined by treatment with 50 μM Aβ-(1–40) either alone or in combination with 1 nM TGF-βs (R&D Systems) for 72 h. The reverse peptide, Aβ-(40–1), was used as a peptide control. Mitochondrial function, as an index of cell viability, was monitored using the 3-(4,5-dimethylthiazol-2-yl)-2,5-diphenyl tetrazolium (MTT) dye conversion assay. MTT (20 μl of a 5 mg/ml solution in sterile phosphate-buffered saline) was added to the cells and allowed to incubate for 3 h at 37 °C. The reaction was terminated by addition of 20% SDS in water/*N*,*N*-dimethylformamide (1:1), pH 4.7. Optical density was measured at 590 nm.

Surface Plasmon Resonance—Between 1200 and 1600 resonance units of Aβ peptides [*e.g.* Aβ-(1–40), Aβ-(25–35), and Aβ-(12–28)] were immobilized using the standard amine-coupling procedure onto CM5 sensor chips which were docked in a Surface Plasmon Resonance-based biosensor (BIAcore™; Biosensor AB, Uppsala, Sweden). Briefly, an injection of 50 μl of NHS/EDC was followed by manual injection at a flow rate of 5 μl/min of freshly prepared Aβ peptide diluted to 25 μg/ml in 10 mM acetic acid (pH 4.0). The remaining active sites on the surface were blocked by injection of 50 μl ethanolamine (pH 8.0). Binding curves were obtained by injecting fresh solutions of TGF-β1 or TGF-β2 (12.5–150 nM) in Hepes-buffered saline (pH 7.4) over the test surfaces. The binding curves from mock surfaces (no Aβ peptide immobilized) were subtracted from the corresponding experimental curves.

Morphological Characterization of Aβ-(1–40) Fibrils—Aβ-(1–40) was incubated at a concentration of 1 mg/ml (~235 μM) in 50 mM phosphate buffer (pH 7.0) either alone or in combination with 5 μg/ml (~200 nM) of either TGF-β1 or TGF-β2 for 48 h at room temperature without agitation. A small amount of specimen was placed onto 200-mesh Formvar-coated grids, blotted, and then air-dried. The specimen was negatively stained with 1% (w/v) potassium phosphotungstic acid (pH 7.0) prior to examination with a JEM-2000FX electron microscope (JEOL, Ltd., Tokyo, Japan) using an accelerating voltage of 80 kV.

Immunolocalization of TGF-β Receptors in Mouse Hippocampus—Mice (C3H/C57Bl; Charles River Laboratories) were terminated by cervical dislocation, and the brains were quickly removed, frozen in liquid nitrogen and kept at −80 °C until use. Animal maintenance and manipulation was performed according to the recommendations of our ethical committees (Biotechnology Research Institute-NRC). Affinity-purified polyclonal antibodies (Santa Cruz Biotechnology, Inc., Santa Cruz, CA) were used for localization of TGF-β RI (V-22, 2 μg/ml), RII (C-16, 1 μg/ml), and RIII (C-20, 2 μg/ml) receptors. Antibody specificity was confirmed using biosensor and Western blot analyses. Serial sagittal sections (8-μm thick) were incubated with the primary antibody in phosphate-buffered saline/1% bovine serum albumin in a moist chamber overnight at 4 °C. The specificity of the immunoreactions was tested by exclusion of the primary antibody as well as by competition, *i.e.* preblocking the primary antibody with the immunizing peptide (2–5 μM). Following several rinses in phosphate-buffered saline, the sections were incubated for 1 h at room temperature with horseradish peroxidase-conjugated secondary antibody. Antigen expression was visualized (0.3% diaminobenzidine, 0.025% H_2O_2, 2–10 min) by light microscopy. Cell soma were counterstained with methyl green. This series of experiments was repeated 4–6 times using tissue obtained from both male and female mice ranging in age from 7 to 10 months.

Statistics—Data were analyzed by one- or two-way analysis of variance using $p < 0.05$ as the criterion for significance. Post-hoc analysis relied on Dunnet's Multiple Comparisons Test.

RESULTS

Aβ-(1–40) Diminishes ^{125}I-TGF-β1 Labeling of Cell Surface Receptors—Three high affinity cell surface receptors for TGF-β have been identified, *i.e.* the type I, II, and III receptors (RI, RII, and RIII, respectively; Ref. 19). One approach to investigating the mechanism of action of TGF-β on Aβ-mediated effects is to determine the effect of freshly dissolved Aβ on TGF-β binding to these three receptors. We analyzed this using ^{125}I-TGF-β1 binding on Mv1Lu cells which express relatively high levels of these receptors. Analysis of variance of all treatment groups revealed significant reductions in binding of ^{125}I-TGF-β1 to all three types of receptors, *i.e.* RI ($F_{(10, 69)} = 3.853$, $p = 0.0004$), RII ($F_{(10, 56)} = 2.653$, $p = 0.0101$) and RIII ($F_{(10, 69)} = 2.824$, $p = 0.0054$). *Post-hoc* analysis indicated that this effect occurred, in a dose-dependent manner, with the physiologically relevant peptide Aβ-(1–40), but not with the Aβ-(12–28) and Aβ-(25–35) fragments (Fig. 1).

Aβ-(1–40)-mediated Neurotoxicity Is Potentiated by TGF-β Isoforms in a Receptor-independent Manner—To examine the receptor-dependence of TGF-β on Aβ-(1–40)-mediated neurotoxicity, we chose to use cells that do not express TGF-β receptors (*i.e.* PC12 cells) and comparing these to cells that express all three TGF-β receptor types (*i.e.* SH-SY5Y) (Ref. 20 and confirmed in our laboratory). Using PC12 cells eliminates the possibility of any event being obscured by TGF-β RII receptor-mediated neuroprotection (10, 17). We first confirmed the conformation state of freshly dissolved Aβ-(1–40) using circular dichroism. Aβ underwent a well-defined random coil → β-sheet transition (Fig. 2), as expected of a species undergoing a conformational transition associated with fibril formation (18, 21). We used neurite retraction and mitochondrial conversion of the tetrazolium redox dye, MTT, as early indicators of cytotoxicity. TGF-β1 and TGF-β2 alone had no observable effect on either neurite retraction or MTT dye conversion in PC12 cells ($F_{(2, 29)} = 0.3632$, $p = 0.6985$, Fig. 3*A*), as expected of cells that do not express TGF-β receptors. Also as expected, Aβ-(1–40) treatment caused neurite retraction (Fig. 3*A*) and inhibition of MTT dye conversion (reduced by 25% relative to untreated PC12 cells, $t_{0.05,23} = 3.426$, $p = 0.0023$, Fig. 3*B*). Both TGF-β1 and TGF-β2 potentiated the cytotoxic effect of Aβ-(1–40) as evidenced by further neurite retraction (Fig. 3*A*) and a further reduction of MTT dye conversion (to 50% of control, $F_{(2, 19)} = 4.968$, $p = 0.0184$, Fig. 3*B*). Aβ-(1–40) also induced a reduction in MTT dye conversion in SH-SY5Y cells ($F_{(5, 22)} = 24.78$, $p = 0.0001$, Fig. 3*B*), however, this effect was not exacerbated by TGF-βs which is expected of a cell model expressing all three

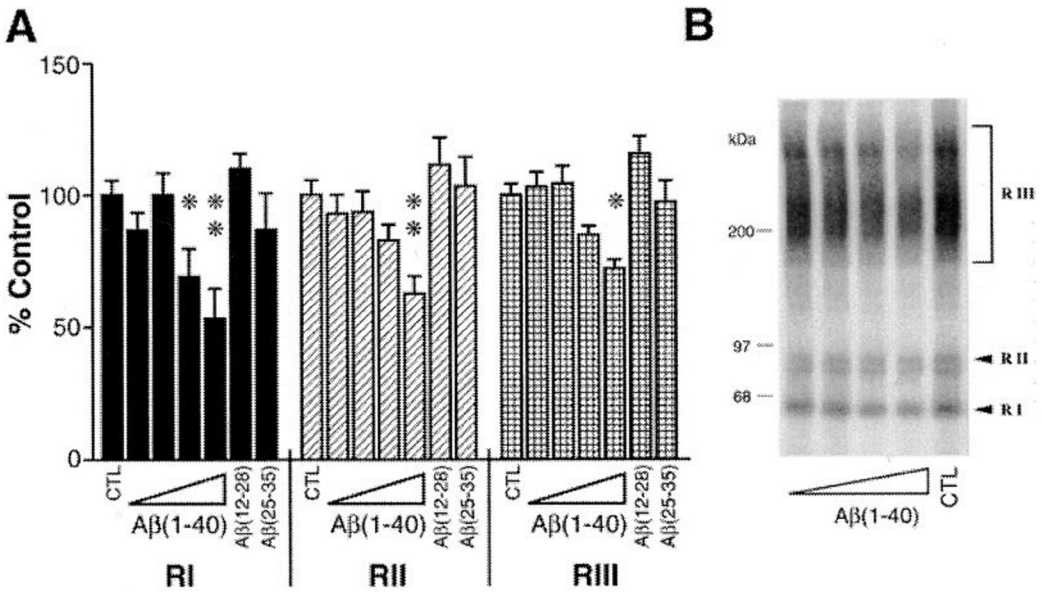

FIG. 1. **Aβ-(1–40) decreases ^{125}I-TGF-β1 binding to Mv1Lu cell surface TGF-β receptors.** *A*, densitometric quantification of TGF-β RI, RII, and RIII receptor binding in the presence of increasing concentrations (1–50 μM) of Aβ-(1–40) is depicted. Experiments included similar concentrations of the pharmacological Aβ fragments, *i.e.* Aβ-(12–28) or Aβ-(25–35); however, only those data corresponding to the 50 μM concentrations of these two fragments are shown. Treatment with Aβ-(1–40), but not the Aβ-(12–28) and Aβ-(25–35) fragments, resulted in significant reductions in ^{125}I-TGF-β1 binding to all three types of TGF-β receptors. Data ($n = 6–8$) are displayed as mean ± S.E. percent control. *, $p < 0.05$ and **, $p < 0.01$ compared with control. *B*, a representative autoradiogram of ^{125}I-TGF-β1-labeled receptors depicts the Aβ-(1–40)-mediated concentration-dependent reduction in binding.

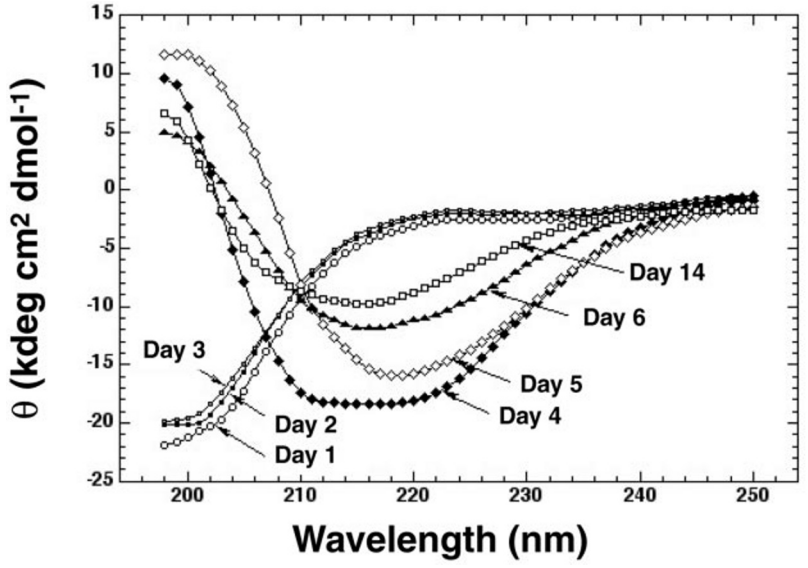

FIG. 2. **Examination of Aβ β-sheet content by circular dichroism.** The secondary structure of Aβ-(1–40) was monitored over a period of 14 days by circular dichroism spectroscopy. Aβ underwent a characteristic random coil → β-sheet transition, as expected of a small Aβ species undergoing fibrillogenesis.

TGF-β receptor types. In fact, a marginal reversal of the effect of Aβ-(1–40) was observed during treatment with TGF-βs. These combined data demonstrate that TGF-β receptor-mediated events supersede the receptor-independent events. The reverse peptide, Aβ-(40–1), did not exert any effect on MTT reduction either alone or in combination with TGF-βs (data not shown). The extremely low ratio of TGF-βs to Aβ-(1–40) used during these experiments, *i.e.* a 1 to 50,000 molar ratio, supports the idea that TGF-β may have a seeding effect and emphasizes the potential physiological relevance of these observations.

TGF-β Isoforms Bind Directly to Aβ-(1–40) with Low Nanomolar Affinities—We used a Surface Plasmon Resonance-based biosensor to test for a direct physical interaction between TGF-β isoforms and Aβ peptides. The biosensor would detect mass accumulation resulting from binding of the individual TGF-β isoforms to the covalently immobilized Aβ peptides as a change in the refractive index of the surface matrix and would generate a curve recorded in arbitrary resonance units (RUs). Both TGF-β1 and TGF-β2 were observed to bind significantly to freshly dissolved Aβ-(1–40), with the binding of TGF-β2 being greater than that of TGF-β1 (Fig. 4, *A* and *B*). The extent of binding of the TGF-β isoforms to Aβ-(12–28) was significantly lower than that observed with Aβ-(1–40), while no detectable binding was observed on surfaces to which Aβ-(25–35) was immobilized. Subsequent biosensor experiments were focused on the physiologically relevant Aβ-(1–40) peptide given the overall lack of interaction of the pharmacological fragments Aβ-(25–35) and Aβ-(12–28) with TGF-β isoforms in the present biosensor study. The specificity of the interaction between injected TGF-β2 and the immobilized Aβ-(1–40) was confirmed by co-injection of the TGF-β ligand specific antibody 3C7 (Celtrix Pharmaceuticals, Inc.) (Fig. 5), thus excluding the possibility that the binding to Aβ-(1–40) that we observed might be

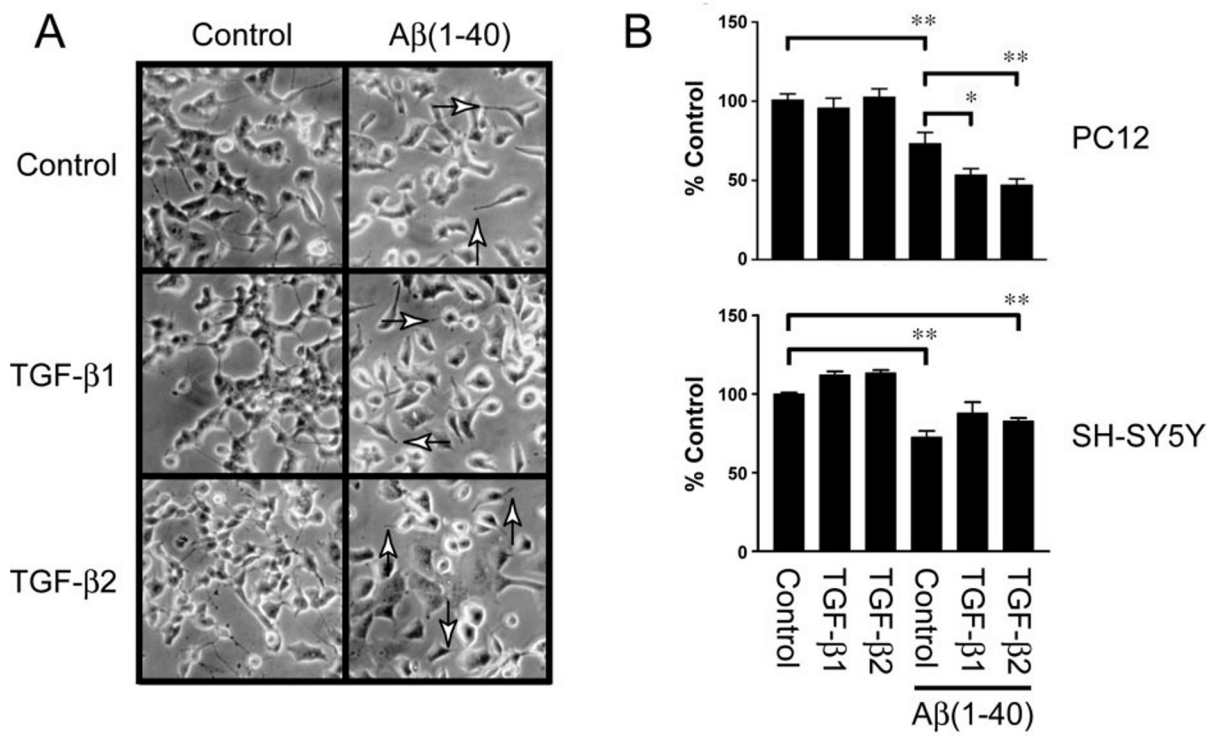

FIG. 3. **TGF-βs enhance Aβ-(1–40)-mediated toxicity in NGF-differentiated PC12 cells.** *A*, the extensive neuritic arborization present in control NGF-differentiated PC12 cell cultures is unaffected by treatment with either TGF-β1 or TGF-β2 (*top*) (original magnification: ×150). Neurite retraction (*arrows*) is readily apparent following treatment with Aβ-(1–40) (*bottom*) and is even more evident following co-treatment with the individual TGF-β isoforms. *B*, the viability of similarly treated PC12 cells was quantitated using MTT dye conversion. Absorbance values (n = 6–8 experiments done in triplicate) are expressed as mean ± S.E. percent control. Aβ-(1–40) reduced MTT dye conversion to ~75% of control levels. TGF-βs alone had no effect on TGF-β receptor-null PC12 cell viability, but they were able to potentiate the toxic effect of Aβ-(1–40) (*top*). In contrast, TGF-βs did not promote the Aβ-(1–40)-mediated toxicity in TGF-β receptor-expressing SH-SY5Y cell culture (*bottom*). The reverse peptide, Aβ-(40–1), did not affect MTT reduction, either alone or in combination with TGF-βs (as these data do not add anything to the figure, they are not shown). **, $p < 0.01$ compared with control and *, $p < 0.05$ compared with Aβ-(1–40) alone.

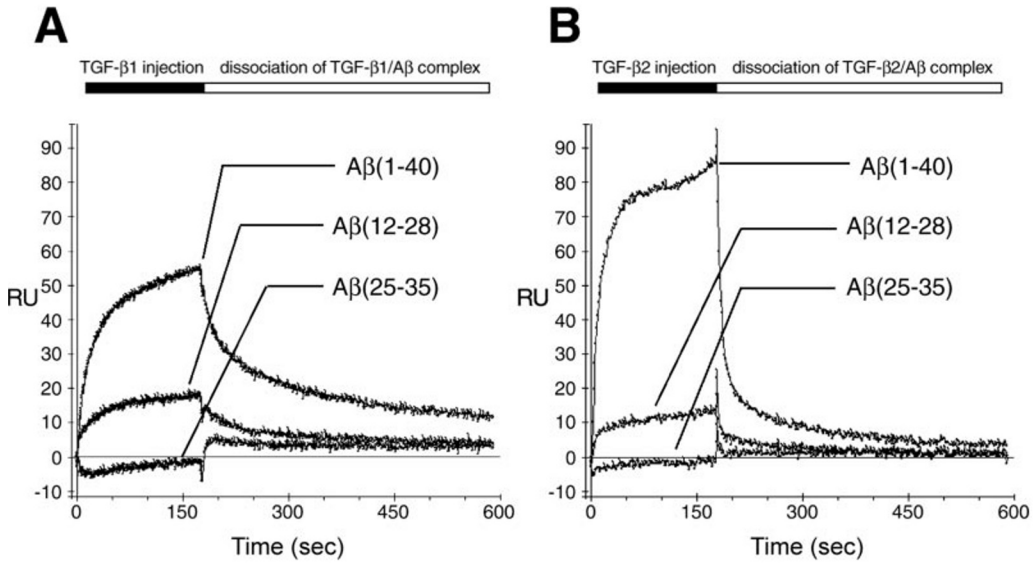

FIG. 4. **TGF-βs interact selectively with Aβ peptides.** The binding of TGF-β isoforms (100 nM) to various Aβ fragments was examined using a Surface Plasmon Resonance-based biosensor. Injection of TGF-β1 (*A*) or TGF-β2 (*B*) over surfaces onto which Aβ-(1–40), Aβ-(12–28), or Aβ-(25–35) were immobilized revealed a significant interaction of both TGF-β isoforms with Aβ-(1–40). A lower affinity interaction between the TGF-β isoforms and the Aβ-(12–28) fragment was also observed, whereas neither isoform recognized the Aβ-(25–35) fragment.

due to a protein contaminant in the commercial TGF-β preparation.

The binding of TGF-β isoforms to freshly dissolved Aβ-(1–40) was characterized in more detail using the biosensor by varying the concentration of TGF-β1 and TGF-β2. The curves (Fig. 6, *A* and *D*) clearly indicated that both TGF-β1 and TGF-β2 bound to Aβ-(1–40) in a concentration-dependent manner. Fitting of these binding data using nonlinear least squares analysis and numerical integration of the differential rate equations (22) demonstrated that the binding of TGF-β1 to Aβ-(1–40) could not be described well by a simple binding model (A+B → AB), as judged by the variance in the residuals

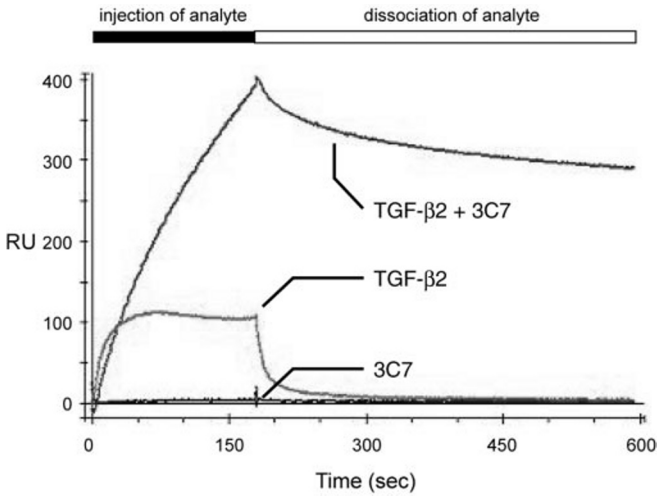

FIG. 5. **Confirmation of the TGF-β-Aβ-(1–40) complex.** Injection of TGF-β2 (100 nM) over the Aβ-(1–40) surface gave the characteristic binding curve. Co-injection of TGF-β2 with the TGF-β ligand specific antibody, 3C7, confirmed the presence of TGF-β2 within the binding complex. Injection of 3C7 alone did not recognize the immobilized Aβ-(1–40).

between the calculated and experimental data (Fig. 6*B*). However, the data was well represented by a rearrangement model (A+B → AB → AB*) (Fig. 5, *A* and *C*) with an apparent K_D of 60.5 ± 5.2 nM. The fitting of the rearrangement model suggests that the initial TGF-β1-Aβ-(1–40) complex undergoes a kinetically detectable rearrangement, perhaps a structural transition. This observation may point to a direct effect of TGF-β1 on Aβ-(1–40) fibril formation since Aβ-(1–40) is known to undergo a conformational transition from a predominantly random coil → β-sheet-rich form during fibrillogenesis. In the case of TGF-β2 (Fig. 6*B*), when the curves derived from all of the TGF-β2 concentrations were taken into account, neither the simple model (Fig. 6E) nor rearrangement model (data not shown) represented the data well. However, the lower concentration curves for TGF-β2 could be fit using a simple model, resulting in an apparent K_D of 96.1 ± 17.9 nM (Fig. 6, *D* and *F*). When the 100 and 150 nM TGF-β2 curves were predicted using the constants derived from the fitting of the lower concentration curves, the experimental curves were found to have significantly higher plateau values than the predicted curves (Fig. 6*D*), illustrating the complexity of the TGF-β2-Aβ-(1–40) interaction. The greater than predicted RU values at higher TGF-β2 concentrations may result from a change in density of the biosensor matrix due to the formation of aggregates or fibrils on the surface. The interaction between TGF-βs and Aβ-(1–40) is not generalized to growth factors. Indeed, this was confirmed by the absence of binding between Aβ-(1–40) and 150 nM nerve growth factor (NGF; data not shown), which, along with TGF-βs, is a member of the cystine-knot-containing superfamily of growth factors (23). Subsequent binding of TGF-β2 to the same surface confirmed the presence of covalently immobilized Aβ-(1–40) (data not shown).

TGF-β Isoforms Promote Aβ-(1–40) Fibril Formation in Vitro—Our biosensor studies confirmed that TGF-βs interact directly with Aβ-(1–40) and suggested a structural transition possibly affecting fibril growth. We used electron microscopy to examine the characteristics of Aβ-(1–40) fibrils formed in the absence and presence of TGF-βs. Lower magnification electron microscopy of Aβ-(1–40) alone showed occasional short strands having a gross morphology characteristic of protofibrils (21) (Fig. 7*a*). In contrast, protofibrils were more abundant and formed network-like assemblies in the Aβ-(1–40) + TGF-β1 (Fig. 7*b*) and Aβ-(1–40) + TGF-β2 (Fig. 7*c*) samples. No detectable structures were discerned with TGF-β1 or TGF-β2 alone (data not shown). The low ratio of TGF-βs to Aβ-(1–40) used during this experiment, *i.e.* a 1–1000 molar ratio, together with our biosensor data indicating a structural transition in the TGF-β-Aβ-(1–40) complex, suggest that TGF-β may enhance fibrillogenesis by generating a conformationally altered form of Aβ-(1–40) with seeding ability. Higher magnification revealed that the Aβ-(1–40) protofibrils were 3–4 nm in width and were composed of a tight helical structure with a periodicity of 2–3 nm based on the coiling of 1 nm wide filaments (Fig. 7, *d–f*). At this magnification, the tight helical nature of the protofibrils was more evident for Aβ-(1–40) + TGF-β2 than for Aβ-(1–40) + TGF-β1, although further magnification of the Aβ-(1–40) + TGF-β1 sample (Fig. 7*e*, *inset*) confirmed the presence of loose helical structures in this sample. This magnification also revealed numerous flexible filaments 1 nm in width in the "interstrand" spaces (data not shown). Interestingly, the morphology of the 3-nm wide helical Aβ-(1–40) protofibrils that predominate in the presence of TGF-β1 and, particularly, TGF-β2 resembles that of *in situ* amyloid protofibrils obtained using advanced sample preparation methods such as cryofixation and freeze substitution (24).

Mouse Hippocampal Field CA1 and Dentate Gyrus Lack TGF-β RI Receptors—The hippocampus is a structure particularly vulnerable during amyloid pathology. The increases in amyloid plaque burden that occur following co-treatment of hippocampal slices with Aβ and TGF-βs (12) and in TGF-β1/hAPP bigenic mice (7, 14) were found to be subfield-specific, indicating the context-dependent nature of TGF-β action. Our observations indicate that TGF-β enhances Aβ-(1–40)-mediated neurotoxicity in a receptor-independent manner. We therefore examined the expression of all three TGF-β receptors within the hippocampal formation to determine if the vulnerability of particular subfields correlates with the pattern of TGF-β receptor expression. Although no TGF-β RI receptor expression was detected in field CA1 and dentate gyrus (Fig. 8*A*), expression was detectable, albeit weak, in the *stratum pyramidale* of fields CA2-CA3, while much stronger staining was found in the *stratum lucidum* of fields CA2-CA3 (Fig. 8*C*) through to the hilus of the dentate gyrus. TGF-β RII receptors were expressed throughout the hippocampal formation particularly in the *stratum pyramidale* of fields CA1-CA3 and the *strata moleculare* and *granulosum* of the dentate gyrus, with sparse staining also observed in the neuropil (Fig. 8, *B* and *D*). We were unable to detect TGF-β RIII receptor expression in the hippocampus. However, examination of the caudate putamen and inner granular layer of the cerebellum revealed diffuse TGF-β RIII receptor staining throughout these regions confirming the ability of this antibody to immunoreact with the TGF-β RIII receptor (data not shown). Experiments were performed in parallel to verify the specificity of the antibodies for the various TGF-β receptors. Competition by preadsorbtion of the antibody with the relevant immunizing peptide diminished immunostaining in all cases (data not shown).

DISCUSSION

The role of TGF-βs in Aβ function has been the subject of much speculation given that it apparently exerts both beneficial and deleterious effects in neuronal cells through the same high-affinity cell surface receptor system (7, 10, 14, 17). We now show that the Aβ-(1–40) peptide decreases ^{125}I-TGF-β1 binding to all three types of TGF-β receptors. These results agree with those of Huang *et al.* (25) who showed that Aβ-(1–40) decreases TGF-β receptor binding but has little effect on TGF-β signaling (confirmed in our laboratory, data not shown), and those of Bodmer *et al.* (26) who also observed that APP does not diminish TGF-β signaling. In explanation of these results,

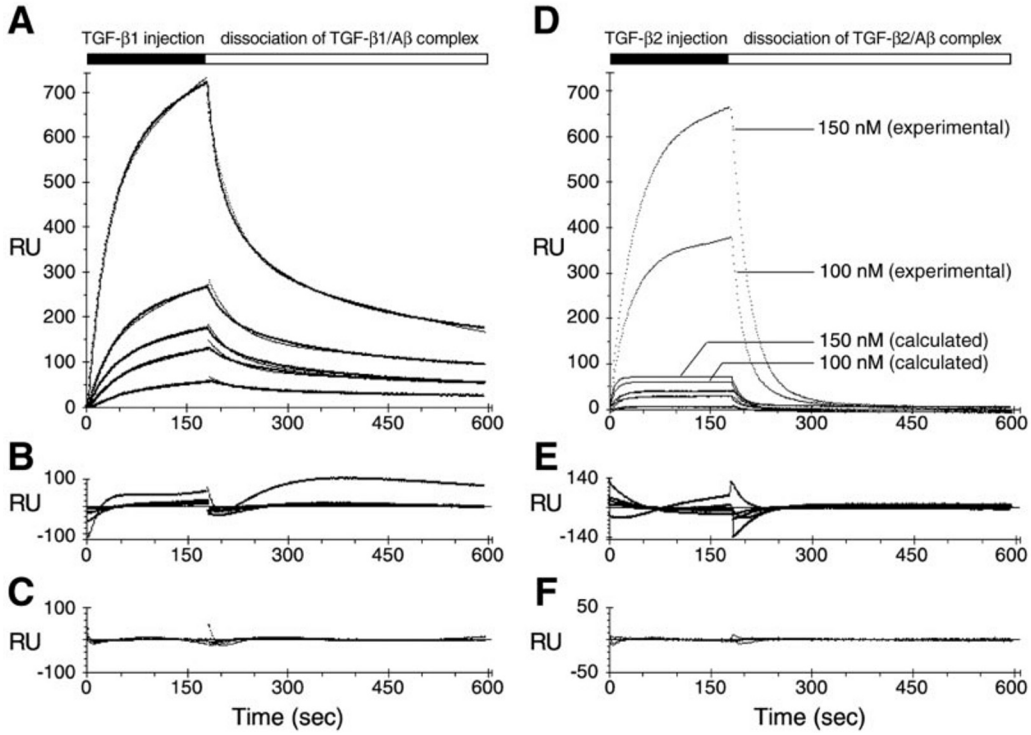

FIG. 6. **TGF-βs interact with Aβ-(1–40) in a complex, concentration-dependent manner.** The binding of increasing concentrations of TGF-β1 (*A–C*) or TGF-β2 (*D–F*) to Aβ-(1–40) was analyzed by Surface Plasmon Resonance. In *panels A* and *D* the experimental curves (points) are shown. In *panels B*, *C*, *E*, and *F* the residuals (difference between calculated and experimental data points) are shown. *Panels A* to *C* indicate that the fit for TGF-β1 is relatively good when using a rearrangement model (*panel C*, S.D. of residuals = 4.65; *panel A*, experimental (points) and calculated (*solid lines*) curves are essentially superimposed) but not when using a simple binding model (*panel B*, S.D. of residuals = 31.21; calculated curves not shown). With respect to TGF-β2 binding, the simple model does not fit all the concentration curves well (*panel E*, S.D. of residuals = 21.99); however, a simple model can be used to fit the three lower TGF-β2 concentration curves (*panel F*, S.D. of residuals = 1.75). Curves for the two higher TGF-β2 concentrations that were predicted using the constants derived from the fitting of the lower three concentration curves are shown for comparison with the experimentally obtained curves (*panel D*).

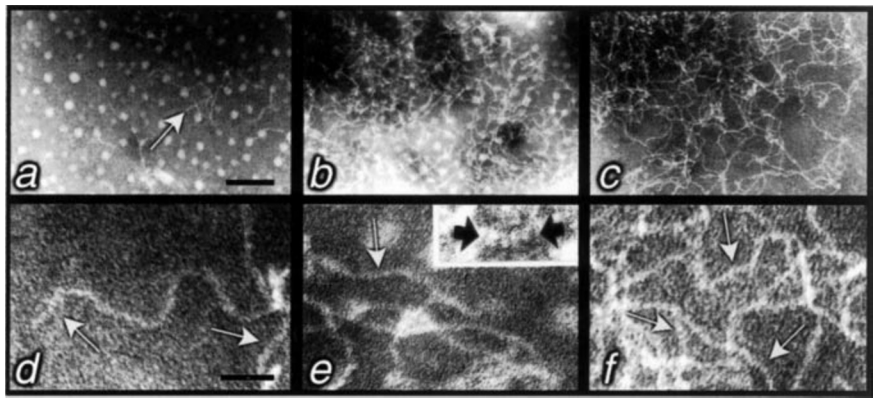

FIG. 7. **Electron micrographs demonstrate TGF-β enhancement of Aβ-(1–40) fibrillogenesis.** Low (*a–c*) and high (*d–f*) magnification views of protofibrils formed after incubation of Aβ-(1–40) alone (*a* and *d*), with TGF-β1 (*b* and *e*), or with TGF-β2 (*c* and *f*). *a*, only a small number of Aβ-(1–40) protofibrils (*arrow*) were observed (*white dots* are artifacts on the supporting film). The protofibrils in *panels b* and *c* are not only more abundant but form a network-like assembly with average openings of ~40 nm. *d–f*, the higher magnification view of Aβ-(1–40) protofibrils indicates that they are 3-nm wide helices (*d*) with a tight helical structure being more readily recognizable in the Aβ-(1–40) + TGF-β2 sample (*f*, *arrows*). Very high magnification confirms the presence of looser helical structures in the Aβ-(1–40) + TGF-β1 sample (*e*, *inset*). Magnification: ×89,100 (*a–c*); ×387,900 (*d–f*); ×707,900 (*e*, *inset*). *Scale bar*; *a–c* = 100 nm, *d–f* = 25 nm.

Huang *et al.* (25) hypothesized that Aβ-(1–40) acts as a classical receptor antagonist, *i.e.* that it interacts directly with a TGF-β receptor. We propose that these binding displacement data are more readily interpreted as resulting from ligand sequestration due to a direct interaction of ligand with Aβ-(1–40) rather than from Aβ-(1–40) interacting with a receptor. Ligand sequestration by Aβ-(1–40) would likely reduce binding to all three receptor types equally, as observed. In contrast, if Aβ-(1–40) was acting as an antagonist at a given receptor type, then it would likely interfere selectively with binding to that receptor type.

In support of our hypothesis, we provide evidence that TGF-β ligands interact directly with Aβ-(1–40) and, at seeding concentrations, enhance the formation of structures having a gross morphology characteristic of protofibrils (Figs. 6 and 7). A tightly coiled or "beaded" substructure reminiscent of the flexible, "beaded" protofibrillar intermediates characterized by Walsh *et al.* (21), was particularly evident when Aβ-(1–40) was coincubated with the TGF-β2 isoform, although a looser helical structure was also observed when Aβ-(1–40) was coincubated with the TGF-β1 isoform (Fig. 7). The pathological relevance of this direct physical interaction was suggested by the ability of

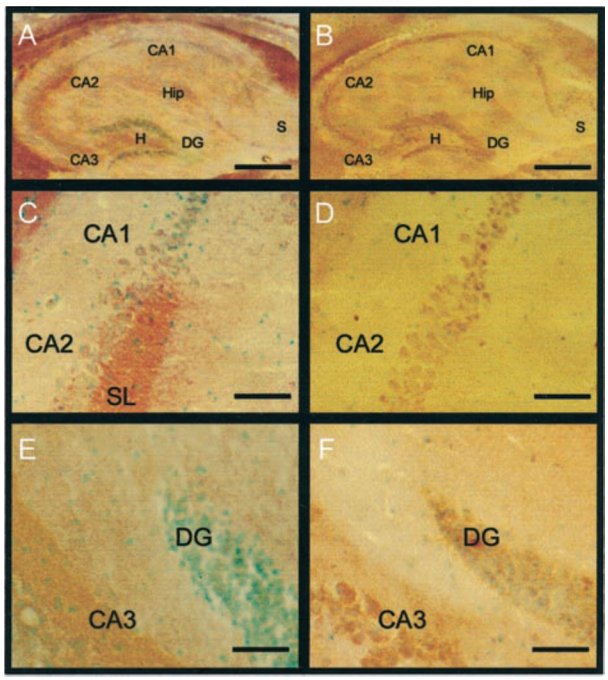

FIG. 8. **TGF-β RI receptors are not expressed in mouse hippocampal field CA1 and dentate gyrus.** *A–D*, sagittal sections of brain obtained from a 10-month old female mouse. TGF-β receptors were immunolocalized using antibody V-22 (*panels A* and *C*; RI receptors) and antibody C-16 (*panels B* and *D*; RII receptors). Immunolocalization was visualized by the secondary antibody-mediated diaminobenzidine coloration. Methyl green was used as the counterstain. TGF-β RI receptor expression was detected in fields CA2-CA3 through to the hilus (*H*) of the dentate gyrus (*DG*), but was conspicuously absent in field CA1 and the DG itself (*A*). In contrast, TGF-β RII receptor expression (*B*) was observed in all subfields of the hippocampus, *i.e.* CA1-CA3, hilus (H) of the dentate gyrus (DG), and subiculum (*S*). Higher magnification (*C–D*) of the CA1-CA2 junction clearly revealed that TGF-β RI immunoreactivity was absent in the *stratum pyramidale* of CA1 (cell soma are stained with methyl green), but present in the *stratum pyramidale* and particularly the *stratum lucidum* (*SL*) of field CA2 (*C*). TGF-β RII immunolocalization demonstrated the presence of staining throughout the CA1 and CA2 (*D*). Similarly, TGF-β RI immunoreactivity was absent in the DG but present in field CA3 (*E*), whereas TGF-β RII immunoreactivity was evident in both CA3 and DG (*F*). *Scale bars*; 500 μm (*A* and *B*), 120 μm (*C* and *D*). *Hip*, hippocampal fissure. These results are representative of at least three separate experiments.

TGF-βs to potentiate Aβ-(1–40)-mediated neurotoxicity in TGF-β-receptor-null PC12 cell culture, but not in SH-SY5Y cell cultures which do express TGF-β receptors (Fig. 3*B*). This receptor-*independent* effect was marginally greater with TGF-β2 than with TGF-β1 (Fig. 3). Ren and colleagues (17) had previously used another TGF-β-receptor null cell culture, *e.g.* NT2/D1, to examine the role of TGF-β in Aβ-function. They did show conclusively that NT2/D1 cells express TGF-β type II receptors upon differentiation, which subserves the neuroprotective effect of TGF-β. However, TGF-βs did not exacerbate Aβ-induced cytotoxicity in undifferentiated NT2/D1 cells. This is easily explained by the fact that these authors made use of the Aβ-(25–35) fragment of Aβ, which does not physically interact with TGF-βs (present study) and, thus, does not allow for our proposed TGF-β receptor-independent events. The importance of TGF-β receptor-independent events is underscored by our demonstration of the low "seeding" ratios of TGF-β to Aβ-(1–40) required to promote Aβ-(1–40) protofibril formation and neurotoxicity. The accumulation and stabilization of protofibrillar populations are believed to be obligate factors in Aβ fibrillogenesis (27). In fact, recent observations suggest that the plaque deposit might simply represent the clinical end point in the Aβ cascade, with most of the neurotoxicity being mediated by smaller oligomeric/protofibrillar conformations (28–31). Several proteins have been shown to codeposit in amyloid plaques and a subset of these appear to modulate Aβ fibrillogenesis (reviewed in Ref. 32). Yet, relatively high ratios of modulator to Aβ are often required for enhancement of fibrillogenesis, and contradictory results have been obtained for the effects of several of these proteins on Aβ fibrillogenesis, putting into question the relevance of these results to the roles of these modulators *in vivo* (see Ref. 33).

Optimal TGF-β receptor-mediated signaling hinges on recruitment of ligand by the TGF-β RIII receptor, subsequent binding to the RII receptor, and transphosphorylation of the RI receptor, the latter event being an absolute requirement for signaling (19, 34). Our demonstration of a lack of detectable RI receptor expression in the hippocampal CA1 pyramidal layer and dentate gyrus (Fig. 8) suggests that signaling from either TGF-β1 or -β2 would not be favored in these two subfields, both of which are vulnerable during amyloid insult (30). We have also previously shown that binding of the TGF-β1 isoform to RII receptors can occur independently of RIII receptors, while binding of the TGF-β2 isoform to RII receptors appears to require RIII receptors (35). Our present demonstration of a lack of detectable TGF-β RIII receptor immunoreactivity in the hippocampus therefore suggests that TGF-β2 binding to receptors would not be favored in this structure, facilitating the interaction of this isoform of TGF-β with Aβ-(1–40). In support of the relevance of the TGF-β2-Aβ interaction to fibrillogenesis and neurotoxicity *in vivo*, it has been observed that the distribution of fibrillar Aβ deposits in brains from two APP transgenic mouse models (36–38) as well as the regional vulnerability of AD brains (39) parallels the regional distribution of TGF-β2 immunoreactivity in mouse (40) and rat (41) brain, *i.e.* frontal and entorhinal cortices and hippocampus. The fact that degenerative changes of the CA1 pyramidal layer induced by co-treatment of hippocampal slices with Aβ and TGF-βs were limited to the TGF-β2 isoform (12) further emphasizes the importance of this isoform in neurodegeneration. Taken together, these receptor localization data support the hypothesis that the direct, receptor-independent effect of TGF-β is an important component of its amyloidogenicity. This molecular mechanism does not mitigate, but rather complements, the regionally selective nature of TGF-β's receptor-*dependent* effect, for example, on extracellular matrix deposition by cerebrovascular cells or on Aβ clearance by parenchymal glial cells. Our present cell culture data suggest that TGF-β receptor-mediated events would supersede the receptor-independent events. One may also speculate as to the possibility of isoform-specific pathologies (*e.g.* TGF-β1 and cerebrovascular amyloid angiopathy & TGF-β2 and AD-like neurodegeneration) based on regional and/or cell-type specific TGF-β isoform and receptor expression (7, 10, 12, 14, 40, 41).

The identification of a receptor-independent interaction between TGF-βs and Aβ defines a molecular mechanism that provides for a potent amyloidogenic action of TGF-β. We suggest that a specific targeting of the Aβ-TGF-β interaction would diminish Aβ protofibril formation, which was recently suggested to be more relevant to neurotoxicity than late stage plaque formation.

Acknowledgments—We thank Drs. A. E. G. Lenferink and J. Zwaagstra for critical review of the article, S. Grothe for help with the biosensor experiments, and A. Migneault for help in preparation of the figures. We wish to thank the Electron Microscopy Center, McGill University (Montreal, Canada) for the use of its facilities.

REFERENCES

1. Selkoe, D. J. (1998) *Trends Cell Biol.* **8,** 447–453
2. Sturchler-Pierrat, C., Abramowski, D., Duke, M., Wiederhold, K. H., Mistl, C.,

Rothacher, S., Ledermann, B., Burki, K., Frey, P., Paganetti, P. A., Waridel, C., Calhoun, M. E., Jucker, M., Probst, A., Staufenbiel, M., and Sommer, B. (1997) *Proc. Natl. Acad. Sci. U. S. A.* **94,** 13287–13292
3. Calhoun, M. E., Burgermeister, P., Phinney, A. L., Stalder, M., Tolnay, M., Wiederhold, K. H., Abramowski, D., Sturchler-Pierrat, C., Sommer, B., Staufenbiel, M., and Jucker, M. (1999) *Proc. Natl, Acad, Sci. U. S. A.* **96,** 14088–14093
4. Schenk, D. (2002) *Nat. Rev. Neurosci.* **3,** 824–828
5. Haass, C. (2002) *Nat. Med.* **8,** 1195–1196
6. Pfeifer, M., Boncristiano, S., Bondolfi, L., Stalder, A., Deller, T., Staufenbiel, M., Mathews, P. M., and Jucker, M. (2002) *Science* **298,** 1379
7. Wyss-Coray, T., Masliah, E., Mallory, M., McConlogue, L., Johnson-Wood, K., Lin, C., and Mucke, L. (1997) *Nature* **389,** 603–606
8. Gupta-Bansal, R., Frederickson, R. C., and Brunden, K. R. (1995) *J. Biol. Chem.* **270,** 18666–18671
9. Castillo, G. M., Ngo, C., Cummings, J, Wight, T. N., and Snow, A. D. (1997) *J. Neurochem.* **69,** 2452–2465
10. Flanders, K. C., Ren, R. F., and Lippa, C. F. (1998) *Prog. Neurobiol.* **54,** 71–85
11. Frautschy, S. A., Yang, F., Calderon, L., and Cole, G. M. (1996) *Neurobiol. Aging* **17,** 311–321
12. Harris-White, M. E., Chu, T., Balverde, Z., Sigel, J. J., Flanders, K. C., and Frautschy, S. A. (1998) *J. Neurosci.* **18,** 10366–10374
13. Lesne, S., Docagne, F., Gabriel, C., Liot, G., Lahiri, D. K., Buee, L., Plawinski, L., Delacourte, A., MacKenzie, E. T., Buisson, A., and Vivien, D. (2003) *J. Biol. Chem.* **278,** 18408–18418
14. Wyss-Coray, T., Lin, C., Yan, F., Yu, G. Q., Rohde, M., McConlogue, L., Masliah, E., and Mucke, L. (2001) *Nat. Med.* **7,** 612–618
15. Prehn, J. H., Bindokas, V. P., Jordan, J., Galindo, M. F., Ghadge, G. D., Roos, R. P., Boise, L. H., Thompson, C. B., Krajewski, S., Reed, J. C., and Miller, R. J. (1996) *Mol. Pharmacol.* **49,** 319–328
16. Ren, R. F., and Flanders, K. C. (1996) *Brain Res.* **732,** 16–24
17. Ren, R. F., Hawver, D. B., Kim, R. S., and Flanders, K. C. (1997) *Mol. Brain Res.* **48,** 315–322
18. Kirkitadze, M. D., Condron, M. M., and Teplow, D. B. (2001) *J. Mol. Biol.* **312,** 1103–1119
19. Massagué, J. (2000) *Nat. Rev. Mol. Cell. Biol.* **1,** 169–178
20. Massagué, J., Cheifetz, S., Boyd, F. T., and Andres, J. L. (1990) *Ann. N. Y. Acad. Sci.* **593,** 59–72
21. Walsh, D. M., Hartley, D. M., Kusumoto, Y., Fezoui, Y., Condron, M. M., Lomakin, A., Benedek, G. B., Selkoe, D. J., and Teplow, D. B. (1999) *J. Biol. Chem.* **274,** 25945–25952
22. De Crescenzo, G., Grothe, S., Lortie, R., Debanne, M. T., and O'Connor-McCourt, M. D. (2000) *Biochemistry* **39,** 9466–9476
23. Wiesmann, C., and de Vos, A. M. (2000) *Nat. Struct. Biol.* **7,** 440–442
24. Inoue, S. (2001) *Int. Rev. Cytol.* **210,** 121–161
25. Huang, S. S., Huang, F. W., Xu, J., Chen, S., Hsu, C. Y., and Huang, J. S. (1998) *J. Biol. Chem.* **273,** 27640–27644
26. Bodmer, S., Podlisny, M. B., Selkoe, D. J., Heid, I., and Fontana, A. (1990) *Biochem. Biophys. Res. Commun.* **171,** 890–897
27. Ramirez-Alvarado, M., Merkel, J. S., and Regan, L. (2000) *Proc. Natl. Acad. Sci. U. S. A.* **97,** 8979–8984
28. Chui, D. H., Tanahashi, H., Ozawa, K., Ikeda, S., Checler, F., Ueda, O., Suzuki, H., Araki, W., Inoue, H., Shirotani, K., Takahashi, K., Gallyas, F., and Tabira, T. (2000) *Nat. Med.* **5,** 560–564
29. Hartley, D. M., Walsh, D. M., Ye, C. P., Diehl, T., Vasquez, S., Vassilev, P. M., Teplow, D. B., and Selkoe, D. J. (1999) *J. Neurosci.* **19,** 8876–8884
30. Klein W. L., Krafft G. A., and Finch C. E. (2001) *Trends Neurosci.* **24,** 219–224
31. Kirkitadze, M. D., Bitan, G., and Teplow, D. B. (2002) *J. Neurosci. Res.* **69,** 567–577
32. McLaurin, J., Yang, D., Yip, C. M., Fraser, P. E. (2000) *J. Struct. Biol.* **130,** 259–270
33. Teplow, D. B. (1998) *Amyloid: Int. J. Exp. Clin. Invest.* **5,** 121–142
34. Blobe, G. C., Schiemann, W. P., Pepin, M. C., Beauchemin, M., Moustakas, A., Lodish, H. F., and O'Connor-McCourt, M. D. (2001) *J. Biol. Chem.* **276,** 24627–24637
35. De Crescenzo, G., Grothe, S., Zwaagstra, J., Tsang, M., and O'Connor-McCourt, M. D. (2001) *J. Biol. Chem.* **276,** 29632–29643
36. Johnson-Wood, K., Lee, M., Motter, R., Hu, K., Gordon, G., Barbour, R., Khan, K., Gordon, M., Tan, H., Games, D., Lieberburg, I., Schenk, D., Seubert, P., and McConlogue, L. (1997) *Proc. Natl. Acad. Sci. U. S. A.* **94,** 1550–1555
37. Irizarry, M. C., Cheung, B. S., Rebeck, G. W., Paul, S. M., Bales, K. R., and Hyman, B. T. (2000) *Acta Neuropathol.* (*Berl.*) **100,** 451–458
38. Holtzman, D. M., Fagan, A. M., Mackey, B., Tenkova, T., Sartorius, L., Paul, S. M., Bales, K., Ashe, K. H., Irizarry, M. C., and Hyman, B. T. (2000) *Ann. Neurol.* **47,** 739–747
39. Arnold, S. E., Hyman, B. T., Flory, J., Damasio, A. R., and Van Hoesen, G. W. (1991) *Cereb. Cortex* **1,** 103–116
40. Flanders, K. C., Ludecke, G., Engels, S., Cissel, D. S., Roberts, A. B., Kondaiah, P., Lafyatis, R., Sporn, M. B., and Unsicker, K. (1991) *Development* **113,** 183–191
41. Poulsen, K. T., Armanini, M. P., Klein, R. D., Hynes, M. A., Phillips, H. S., and Rosenthal, A. (1994) *Neuron* **13,** 1245–1252